

PROCEEDINGS OF SPIE

[SPIDigitalLibrary.org/conference-proceedings-of-spie](https://spiedigitallibrary.org/conference-proceedings-of-spie)

Detecting best lag of embedding for modeling spike-wave discharges from experimental data

Grishchenko, Anastasiya, Sysoeva, Marina, van Rijn, Clementina, Sysoev, Ilya

Anastasiya A. Grishchenko, Marina V. Sysoeva, Clementina M. van Rijn, Ilya V. Sysoev, "Detecting best lag of embedding for modeling spike-wave discharges from experimental data," Proc. SPIE 11459, Saratov Fall Meeting 2019: Computations and Data Analysis: from Nanoscale Tools to Brain Functions, 114590H (9 April 2020); doi: 10.1117/12.2563453

SPIE.

Event: Saratov Fall Meeting 2019: VII International Symposium on Optics and Biophotonics, 2019, Saratov, Russian Federation

Detecting best lag of embedding for modeling spike-wave discharges from experimental data

Anastasiya A. Grischenko^{a,b}, Marina V. Sysoeva^{c,b}, Clementina M. van Rijn^d, Ilya V. Sysoev^{a,b}

^aSaratov State University, 83 Astrakhanskaya str., Saratov, Russia;

^bSaratov Branch of Institute of Radioengineering and Electronics of RAS, 38 Zelenaya str., Saratov, Russia;

^cYuri Gagarin State Technical University of Saratov, 77 Politechnicheskaya str., Saratov, Russia;

^dRadboud University Nijmegen, Donders Centre for Cognition, Nijmegen, The Netherlands.

ABSTRACT

Purpose. Optimal value of the embedding lag calculation is made. Lag is one of empirical parameters of mathematical models, used in autoregressive models for prediction, coupling analysis, signal classification etc.

Methods. The first minimum in the dependence of the mutual information function on the time lag was detected.

Results. The calculation showed that the optimal lag is about 8 sampling intervals (1/64 s or 1/8 of the characteristic oscillation period for the absence seizures).

Discussion. The optimal lag is about 1/8 of the characteristic oscillation period was obtained for both epileptiform and background activity, including preictal and different stages of ictal activity, i. e. this time scale is present in the signal throughout the observation time.

Keywords: epilepsy, predictive model, embedding lag, time series analysis, local field potentials

1. INTRODUCTION

Generalized spike-wave discharges (SWD) are formed due to dysfunction of the thalamo-cortical system. They are an electroencephalographic sign of absence epilepsy. Absence epilepsy is a widespread among children and adolescents (up to 50% of the total number of cases of all types of epilepsy) form of epilepsy, which etiology is not completely clear. The main manifestations of absentee epilepsy are partial or complete losses of consciousness for a short time.

Patients with absence epilepsy do not have indications for invasive studies and surgical interventions. This limits the possibilities of acquisition of information about the neurobiological mechanisms of this disease. Therefore, experimental work is traditionally carried out on rats of two inbred lines with a genetic predisposition to absence epilepsy: GAERS and WAG/Rij.¹⁻⁴ Pharmacological, behavioral and electroencephalographic signs of absence epilepsy in them are similar to those in humans.⁵⁻⁷

For humans, the main oscillation frequency during SWD decreases from 5 Hz at the beginning to 3 Hz at the termination, the seizure duration has an average of 5–6 s. In GAERS rats, the main frequency decreases during the seizure from 8 Hz to 7 Hz, the average seizure duration is 15 s. In WAG/Rij rats, the sharpest drop in the main oscillation frequency is observed — from 11 Hz to 8 Hz during the first 1 s of the discharge, the average seizure duration is 8 s.⁸

Application of various measures and criteria of nonlinear dynamics and mathematical statistics to electroencephalograms of patients suffering from various pathologies has a long history.⁹ From the point of view of nonlinear dynamics, the electroencephalogram is nothing but an experimental time series. In some problems

Further author information: (Send correspondence to Anastasiya A. Grischenko)
Anastasiya A. Grischenko: E-mail: vili_von@mail.ru

such as: determination of connections between different EEG channels,¹⁰⁻¹³ series clustering,¹⁴ diagnostics of interaction between the central nervous system and the motor system,¹⁵ separation of pathologies and norms and others, it is useful to build an empirical mathematical model from experimental time series. If the properties of the experimental data are used to specify the model parameters and the nonlinear function form, then significantly fewer coefficients will be needed, which will increase the estimation reliability. Also, a smaller time series length can be used to build a model. This in turn makes it possible to have a higher temporal resolution when observing changes in signal characteristics over time. The above is essential for biosignals where the stationarity time is limited.

The purpose of this work is to calculate the optimal value of the embedding lag, which is one of empirical parameters of mathematical models, used in autoregressive models for prediction, coupling analysis, signal classification etc.

2. METHODS

2.1 ANIMALS AND DATA

In this work, 130-minute recordings of intracranial EEG (signals of local field potentials, LFPs) from 6 male WAG/Rij rats were analyzed, 2 experimental recordings from different experiments were considered for each animal, with 28 seizures for each animal in each experiment. All seizures were spontaneous. The data were obtained at a sampling rate of 512 Hz and recorded by a 16-bit ADC with hardware filtering in the 1-99 Hz range and suppression of 50 Hz interference. Four channels corresponding to the hippocampus (Hp; AP -3.5; L 2; depth 3.5), parietal cortex (PC; AP -1.6; L 4), frontal cortex (FC; AP 3.5; L 3) and occipital cortex (OC; AP -6; L -3.5) cortex were recorded. The position of all electrodes was verified histologically.

The length of the selected seizures was at least 6 s. Six intervals (epochs) of 2 s length were extracted from each seizure with surrounding in time activity (table 1). The analysis was performed for each epoch. For convenience, the seizure onset time is considered as 0 s and the seizure termination is taken as T s. These epochs were selected in accordance with the results reported in.¹⁶ Preictal activity is at this time, as a rule, changes in connectivity leading to seizure initiation are detected already.^{17,18} Decoupling is this interval corresponds mainly to the moment of decoupling found in.¹⁶

Table 1. The analyzed epochs

Epoch	Time interval
background activity	[-5; -3] s before the seizure onset
preictal activity	[-2; 0] s before the seizure onset
decoupling	[0; 2] s after the seizure onset
seizure maintenance	[2; 4] s after the seizure onset
postictal stage	[T; T + 2] s after the seizure termination
termination	[T - 2; T] s before the seizure termination

The time series of recording intracranial EEG for the parietal cortex is shown in fig. 1.

2.2 FORECASTING MODEL

Since the time series containing the absence seizures are quite short and irregular (see Fig. 1), it was decided to construct models in the form of model maps (Eq. 1) rather than differential equations:

$$x'_{n+\tau} = f(x_n, x_{n-l}, \dots, x_{n-(D-1)l}), \quad (1)$$

where $\mathbf{x}_n = (x_n, x_{n-l}, \dots, x_{n-(D-1)l})$ is a state vector reconstructed by means of the method of delays,¹⁹⁻²¹ which is a classical approach to transpose time series in phase space, i. e. to obtain the high-dimensional state vector from the scalar time series (black points in fig. 2) $\{x_n\}_{n=1}^N$ for each time point, $x'_{n+\tau}$ is the predicted value (grey star is in fig. 2) corresponding to the measured value $x_{n+\tau}$ (triangle is in fig. 2), f is approximating function (polynomial of the order P in our case), τ is the length of prediction interval (prediction length), i. e., the time

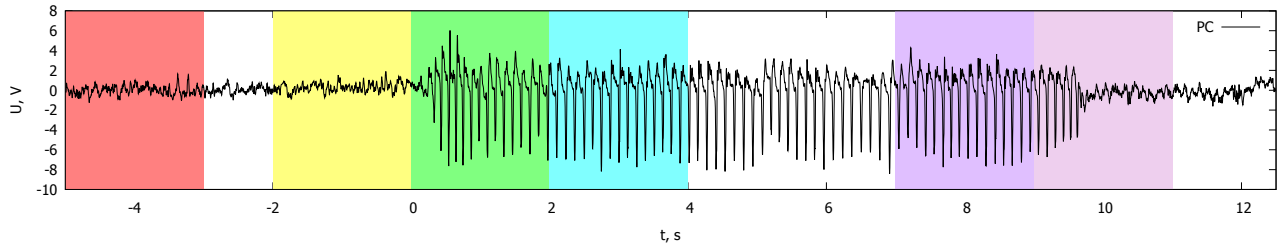


Figure 1. The time series of local field potentials from the parietal (somatosensory) cortex (signal of rat No. 6 is used). The colored background indicates the intervals studied in the work: Red $[-5; -3]$ s before the seizure onset (background activity); Yellow $[-2; 0]$ s before the seizure onset (preictal activity); Green $[0; 2]$ s after the seizure onset (decoupling); Blue $[2; 4]$ s after the seizure onset (seizure maintenance); Dark Purple $[T - 2; T]$ s before the seizure termination; Purple $[t; T + 2]$ s after the seizure termination (postictal stage).

lag between the last point used for vector reconstruction and predicted point, D is embedding dimension that is actually the number of components in a state vector, l is a time delay (or lag), i. e. time interval between EEG values is used to construct the state vector.

Model coefficients are estimated using the least-squares routine²² by minimizing the squared prediction error, that measures the difference between the predicted values $x'_{n+\tau}$ and the observed ones $x_{n+\tau}$. In this example model parameters are: $\tau = 12, l = 5, D = 5$.

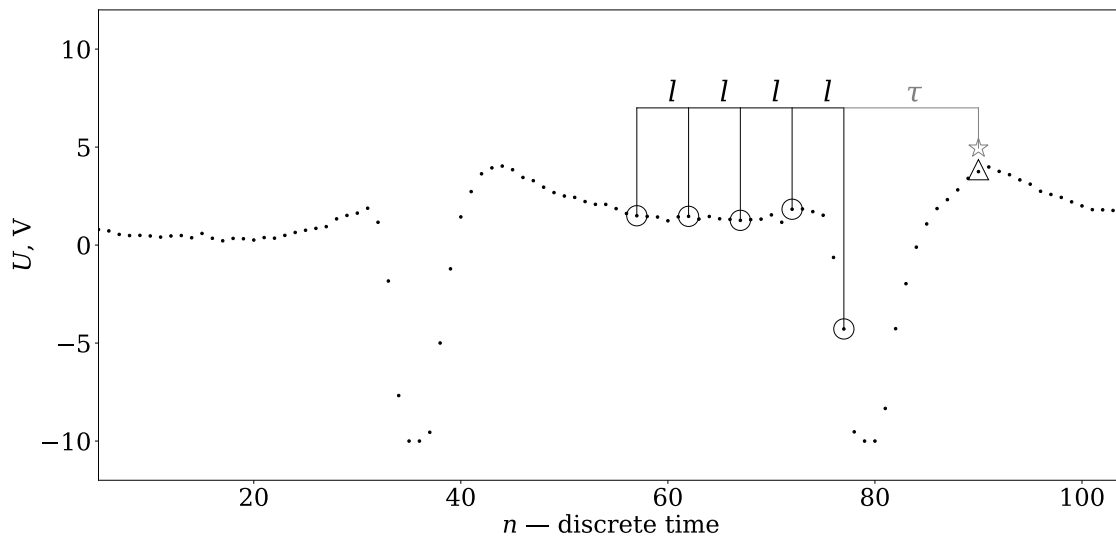


Figure 2. Time series plot with absence seizure, where parameters of adapted nonlinear model are shown. Points of time series $\{x_n\}_{n=1}^N$ are marked with black dots. The point to be predicted $x_{n+\tau}$ is marked with a triangle. The predicted by model value $x'_{n+\tau}$ is marked by a gray star. Points used for prediction (state vector components) are marked with circles. Notation: l is embedding lag, τ is a prediction length. In this example model parameters are: $\tau = 12, l = 5, D = 5$.

This work aims to find the optimal value of the embedding lag for state vector reconstruction from time series of WAG/Rij rats at the seizure. Previously, the optimal lag has already been estimated using the BIC²³ together with the optimal model dimension and the optimal polynomial order¹⁸ and in combination with the prediction length.²⁴ Here we offer another approach for independent selection of the optimal lag and compare results of this approach to previous ones.

2.3 OPTIMAL LAG

It was shown¹⁹ that when reconstructing a state vector over scalar time series, the optimal way to determine the embedding lag is to select it as the first local minimum based on the dependence of the mutual information function of the experimental series on itself shifted in time. Therefore, in this paper, in each case (animal, record number, epoch), different lags were considered in the range from zero to the half of the characteristic period. Then, the value corresponding to the first minimum of $I_{x,y}(l)$ was chosen.

The mutual information function $I_{x,y}$ between two samplings (in our case — time series) $\{x_n\}_{n=1}^N$ and $\{y_n\}_{n=1}^N$ characterizes the degree of series similarity. Applied to the same series with a shift when $y_n = x_{n-l}$, the function shows how quickly the system forgets its past state. There are several approaches to calculation $I_{x,y}$. We used a relatively modern approach proposed in,²⁵ which is based on the counting nearest neighbors of the point in (X, Y) plane. This approach is known to have the least demands on the data volume, which is important in the study of non-stationary physiological signals by nature. The final formula (2) to estimate the mutual information function is as follows:

$$I_{x,y} = \psi(N) + \psi(1) - \langle \psi(n_x(i) + 1) + \psi(n_y(i) + 1) \rangle_i, \quad (2)$$

where N is the series length, $n_x(i)$ and $n_y(i)$ are the number of neighbors of the i -th point on the plane (X, Y) , $\psi(n)$ is the digamma function.

Since the method has a significant computational complexity, a sorting algorithm²⁶ was used.

3. RESULTS

The first minimum in the dependence of the mutual information function on the time lag was detected. Further, the histogram of frequencies for the first minima of the function $I_{xy}(l)$ depending on the l was plotted for each epoch for all records of all studied animals for the four studied channels (see Fig. 3). It is worth noting that such histograms were also built separately for different records for different animals, and they look very similar to the cumulative histogram plotted in Fig. 3. This means that the results for all animals are very close.

Six subfigures of Fig. 3 correspond to 6 different considered epochs (see Fig. 1): background, preictal, onset, maintenance, termination, and postictal. On the X-axis, the step at which the first minimum of the mutual information function is reached is plotted, i. e. the desired optimal model lag is postponed. On the Y-axis, the frequency is deferred.

The calculated histogram showed that the optimal lag is about 8 sampling intervals (1/64 s or 1/8 of the characteristic oscillation period for the absence seizures). This result was obtained for both epileptiform and background activity, including preictal and different stages of ictal activity, i. e. this time scale is present in the signal throughout the observation time.

4. DISCUSSION

Earlier,²⁷ it was shown that for records containing absence seizures, the optimal embedding lag for empirical modeling can be estimated as $l = \Theta/10$, where Θ is the characteristic oscillation period. This result was obtained using the BIC²³ together with the optimal model dimension and the model polynomial order as a result of the single procedure.

Then,²⁴ it was shown that the optimal lag is related to the prediction length. And when choosing a prediction length close to $\Theta/4$, the optimal lag should be equal to $l = \Theta/12$. In that work, the selection was made not aiming forecast as a goal, but immediately for the Granger causality method, which used these predictive models, considering sensitivity and specificity of the coupling analysis as a primary goal. For this, special criteria have been developed.

In this paper, the optimal model lag was selected according to the first minimum of the mutual information function, which theoretically should lead to the fact that the state vector used in the construction of an individual model for the studied time series contains maximum information about the object. As a result, the value of the optimal lag $l = \Theta/8$ was obtained. Nevertheless, it can be seen that all the estimates obtained by different methods for lag are quite close.

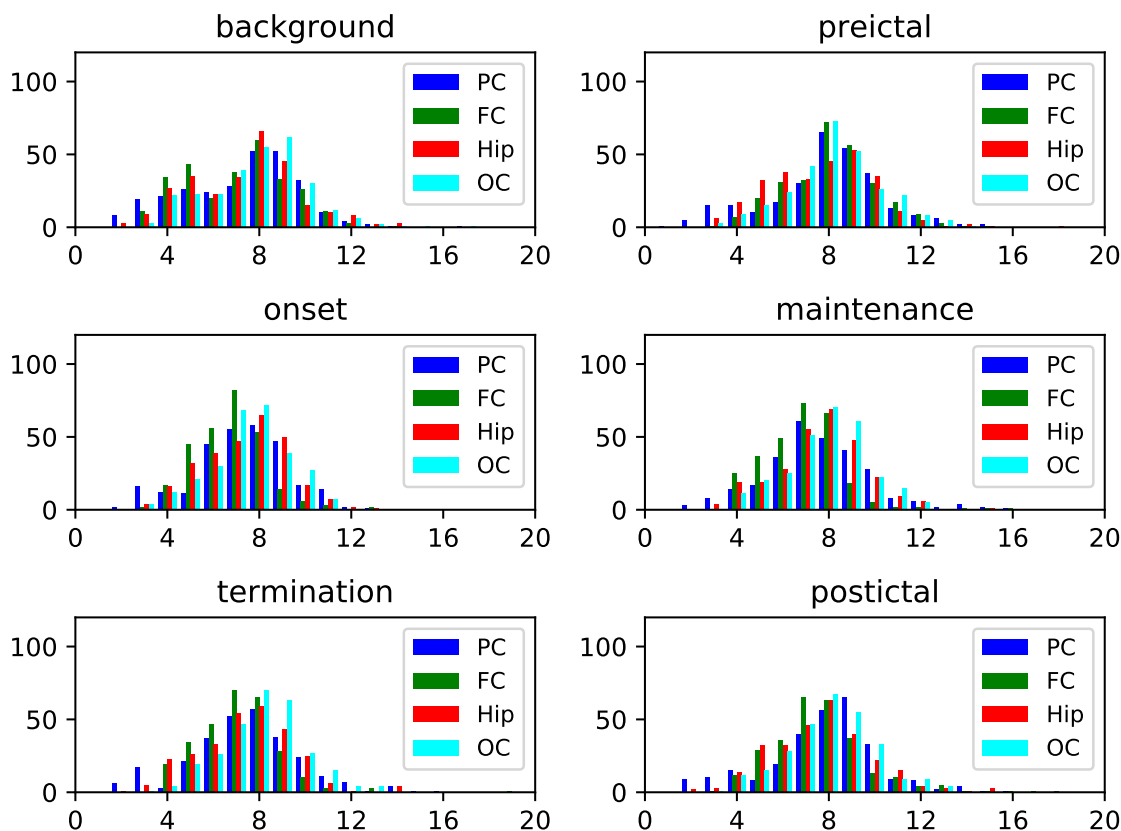


Figure 3. Histogram of frequencies for the first minimum of the mutual information function. X-axis: the step at which the first minimum of the mutual information function is reached. Y-axis: the frequency (number of times reached) for the first minimum. Each subfigure corresponds to one of the time intervals: background, preictal, onset, maintenance, termination, and postictal.

5. ACKNOWLEDGEMENTS

This research was supported by Russian Science Foundation, Grant No. 19-72-10030.

REFERENCES

- [1] C. Marescaux, M. Vergnes, and A. Depaulis, "Genetic absence epilepsy in rats from Strasbourg – a review," *Journal of Neural Transmission (Supplementum)* **35**, pp. 37–69, 1992.
- [2] M. Vergnes, C. Marescaux, A. Depaulis, G. Micheletti, and J. M. Warter, "Spontaneous spike and wave discharges in thalamus and cortex in a rat model of genetic petit mal-like seizures," *Experimental Neurology*, **96**, pp. 127–136, 1987.
- [3] A. Coenen and E. L. J. M. van Luijtelaar, "Genetic animal models for absence epilepsy: a review of the WAG/Rij strain of rats," *Behavior Genetics* **33**, pp. 635–655, 2003.
- [4] A. Depaulis and G. van Luijtelaar, "Genetic models of absence epilepsy in the rat," in *Animal models of seizures and epilepsy*, A. Pitkanen, S. Moshe, and P. Schwartzkroin, eds., pp. 223–248, San Diego: Elsevier Inc., 2006.
- [5] H. Meeren, J. Pijn, E. van Luijtelaar, A. Coenen, and F. Lopes da Silva, "Cortical focus drives widespread corticothalamic networks during spontaneous absence seizures in rats," *J. Neurosci* **22**, pp. 1480–1495, 2002.
- [6] E. Sitnikova, T. V. Dikanav, D. A. Smirnov, B. P. Bezruchko, and G. van Luijtelaar, "Granger causality: cortico-thalamic interdependencies during absence seizures in WAG/Rij rats," *J Neurosci Methods* **170**(2), pp. 245–254, 2008.

- [7] G. van Luijtelaar, E. Sitnikova, and A. Lüttjohann, “On the origin and suddenness of absences in genetic absence models,” *Clin EEG Neurosci* **42** (2), pp. 83–97, 2011.
- [8] O. Akman, T. Demiralp, N. Ates, and F. Onat, “Electroencephalographic differences between WAG/Rij and GAERS rat models of absence epilepsy,” *Epilepsy Research* **89**, pp. 185–193, 2010.
- [9] J. Timmer, S. Haussler, M. Lauk, and C.-H. Lucking, “Pathological tremor: deterministic chaos or nonlinear stochastic oscillators,” *Chaos* **10**(1), pp. 278–288, 2000.
- [10] D. Y. Takahashi, L. A. Baccala, and K. Sameshima, “Connectivity inference between neural structures via partial directed coherence,” *Journal of Applied Statistics* **34**(10), pp. 1255–1269, 2007.
- [11] A. Brovelli, M. Ding, A. Ledberg, Y. Chen, R. Nakamura, and S. Bressler, “Beta oscillations in a large-scale sensorimotor cortical network: Directional influences revealed by Granger causality,” *PNAS* **101**, pp. 9849–9854, 2004.
- [12] R. Vicente, “Transfer entropy—a model-free measure of effective connectivity for the neurosciences,” *Journal of Computational Neuroscience* **30**(1), pp. 45–67, 2011.
- [13] V. A. Vakorin, B. Misic, O. Krakovska, G. Bezgin, and M. A. R., “Confounding Effects of Phase Delays on Causality Estimation,” *PLoS ONE* **8**(1), p. e53588, 2013.
- [14] T. Dikanev, D. Smirnov, R. Wennberg, J. Perez Velazquez, and B. B., “EEG nonstationarity during intracranially recorded seizures: statistical and dynamical analysis,” *Clinical Neurophysiology* **116**, pp. 1796–1807, 2005.
- [15] B. P. Bezruchko, V. I. Ponomarenko, M. D. Prokhorov, D. A. Smirnov, and P. A. Tass, “Modeling nonlinear oscillatory systems and diagnostics of coupling between them using chaotic time series analysis: applications in neurophysiology,” *Physics-Uspekhi* **51**, pp. 304–310, 2008.
- [16] M. V. Sysoeva, A. Lüttjohann, G. van Luijtelaar, and I. V. Sysoev, “Dynamics of directional coupling underlying spike-wave discharges,” *Neuroscience* **314**, pp. 75–89, 2016.
- [17] A. Lüttjohann and G. van Luijtelaar, “The dynamics of cortico-thalamo-cortical interactions at the transition from pre-ictal to ictal LFPs in absence epilepsy,” *Neurobiology of Disease* **47**, pp. 47–60, 2012.
- [18] M. V. Sysoeva, E. Sitnikova, I. V. Sysoev, B. P. Bezruchko, and G. van Luijtelaar, “Application of adaptive nonlinear Granger causality: Disclosing network changes before and after absence seizure onset in a genetic rat model,” *J Neurosci Methods* **226**, pp. 33–41, 2014.
- [19] N. Packard, J. Crutchfield, J. Farmer, and R. Shaw, “Geometry from a Time Series,” *Phys. Rev. Lett.* **45**, pp. 712–716, 1980.
- [20] A. S. Gonchenko, S. V. Gonchenko, A. O. Kazakov, and A. D. Kozlov, “Mathematical theory of dynamical chaos and its applications: review part 1,” *Izvestiya VUZ. Applied Nonlinear Dynamics* **25**(2), pp. 4–36, 2017.
- [21] S. V. Gonchenko, A. S. Gonchenko, A. O. Kazakov, and B. T. V. Kozlov, A. D., “Mathematical theory of dynamical chaos and its applications: Review Part 2. Spiral chaos of three-dimensional flows,” *Izvestiya VUZ. Applied Nonlinear Dynamics* **27**(5), pp. 7–52, 2019.
- [22] A. M. Legendre, *Appendice sur la méthodes des moindres carrés. Nouvelles méthodes pour la détermination des orbites des comètes*, Firmin-Didot, 1805.
- [23] G. Schwarz, “Estimating the dimension of a model. Annals of Statistics,” *Annals of Statistics* **6** (2), pp. 461–464, 1978.
- [24] M. V. Kornilov, T. M. Medvedeva, B. P. Bezruchko, and I. V. Sysoev, “Choosing the optimal model parameters for granger causality in application to time series with main timescale,” *Chaos, Solitons & Fractals* **82**, pp. 11–21, 2016.
- [25] A. Kraskov, H. Stögbauer, and P. Grassberger, “Estimating mutual information,” *Physical Review E* **69**, p. 066138, 2004.
- [26] A. S. Zemljannikov and I. V. Sysoev, “Diagnostics and correction of systematic error while estimating transfer entropy with k-nearest neighbours method,” *Izvestiya VUZ. Applied Nonlinear Dynamics* **23**(4), pp. 24–31, 2015.
- [27] M. V. Sysoeva, T. V. Dikanev, and I. V. Sysoev, “Selecting time scales for empirical model construction,” *Izvestiya VUZ. Applied Nonlinear Dynamics* **20**(2), pp. 54–62, 2012.